Photodisintegration of He^3†

J. R. STEWART, R. C. MORRISON, AND J. S. O'CONNELL*
Electron Accelerator Laboratory, Yale University, New Haven, Connecticut
(Received 7 December 1964)

The $He^3(\gamma,d)p$ differential cross section at 90° in the laboratory system has been measured in the gamma-ray energy range of 8.5 to 46 MeV. A broad peak with a maximum of 93 μb/sr at 11 MeV is observed. A theory of Gunn and Irving (for a radius parameter of 2.7 F) gives a good fit to the measured cross section. When compared with other experiments, the present data agree well with the 90° data of Berman *et al.* and Finckh *et al.* Taking into account angular-distribution corrections, they agree within statistics with the total cross section of Gorbunov *et al.* The $He^3(\gamma,2p)n$ proton energy spectrum produced by 40-MeV bremsstrahlung has also been measured. This spectrum is found to disagree in magnitude with predictions from theories by Gunn and Irving, and by Delves. The spectrum agrees fairly well with that expected from the $He^3(\gamma,2p)n$ cross section measured by Gorbunov *et al.* A survey of sum-rule predictions is also included.

I. INTRODUCTION

THE photodisintegration of He^3 can proceed through two reactions

$$He^3(\gamma,d)p, \quad Q=-5.49 \text{ MeV};$$
$$He^3(\gamma,2p)n, \quad Q=-7.72 \text{ MeV}.$$

In the present experiment, the 90° spectra of the protons and deuterons produced by a fixed end-point bremsstrahlung spectrum are measured. The two-body kinematics of the first reaction permit the initiating gamma-ray energy to be inferred from a measurement of the deuteron energy. The two-body cross section can then be derived with a knowledge of the bremsstrahlung spectrum. In the three-body breakup the kinematics cannot be determined by a measurement of the energy of only one proton. The proton energy spectrum can be compared, however, with the predictions of a theory of the three-body cross section and proton energy distribution.

Section II describes the experimental arrangement. Section III describes the data analysis and concludes with the experimental results. The data are compared with other experimental results in Sec. IV and with various theories in Sec. V. A survey of sum-rule predictions is made in Sec. VI.

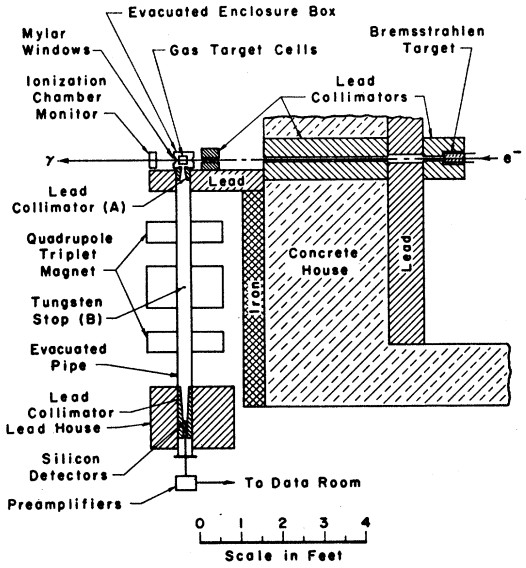

FIG. 1. A plan view of the experimental area. Two gas target cells of He^3 and H^2 were alternately placed in the bremsstrahlung beam by remote control. Collimator (A) was $\frac{1}{2}$-in. in diameter giving ~30% full-width-at-half-maximum energy transmission by the magnet. The stop (B), $\frac{1}{2}$ in. in diameter, was used to eliminate particle trajectories near the magnet axis and to provide detector shielding against soft photons from the target.

II. EXPERIMENTAL ARRANGEMENT

Figure 1 shows a plan view of the experimental arrangement. The Yale electron linac produced a 16-kW beam (400 mA for 5 μsec, 200 times/sec at 40 MeV) which produced bremsstrahlung in a 6-in.-thick aluminum target. The bremsstrahlung was collimated to give a $\frac{3}{4}$-in.-diam beam at the sample. To obtain data for cross sections above 30-MeV gamma energy, the electron beam energy was raised to about 55 MeV.

The target consisted of two similar gas cells $1\frac{1}{2}$ in. in diameter by 2 in. in length, which could be moved in and out of the beam by remote control. One cell was fitted with a 0.00025-in. Havar[1] window at 90° to the beam and filled with 3 atm of H^2. The other cell had Mylar windows of either 0.00014 or 0.00050 in. filled with $\frac{1}{2}$ or $1\frac{1}{3}$ atm, respectively, of He^3. Both the He^3 and H^2 gases were found by a mass spectrometer to be better than 99.5% pure. The He^3 purity was maintained by passing the gas between runs over sodium zeolite at liquid-nitrogen temperature to remove impurities. The H^2 gas was changed between runs.

Charged particles emitted at 90° to the beam in the laboratory were collected by a quadrupole-triplet magnet with a 4-in. aperture, and focused upon silicon detectors. A $\frac{1}{2}$-in.-diam magnet entrance collimator at the target cell and a $\frac{1}{2}$-in.-diam stop in the center of the center magnet limited the momentum transmission

† Work supported by the U. S. Atomic Energy Commission.
* Present address: National Bureau of Standards, Washington, D. C.

[1] Havar is a product of the Precision Metals Division of Hamilton Watch Company, Lancaster, Pennsylvania.

curve to ±7.5%. This corresponds to full width at half-maximum of about 30% in energy. The solid angle at the peak of the transmission curve (solid angle versus momentum) was about 0.01 sr. The properties of this magnet are described elsewhere in more detail.[2] The horizontal angular acceptance of the quadrupole was ±3° centered at 90° (lab). The energy separation of the protons and deuterons from He^3 at one particular magnet setting is shown in the pulse-height spectrum from a silicon detector in Fig. 2. The pulses from the silicon detectors were amplified by a charge-sensitive pre-amplifier and a delay-line-clipped amplifier with a 0.7-μsec clipping time and then stored in a 200-channel analyzer.

A number of silicon semiconductor detectors with depletion depths ranging from 0.045 to 3.0 mm were used either singly or in combinations of two to separate protons and deuterons from the background due to electrons and neutrons.

The background cutoff energy was roughly proportional to the detector thickness and independent of the magnet setting. Since the magnet limited the energy range of incident particles, detector thicknesses less than the particle range could be used. Both the high- and low-energy detection limits were determined by the steeply rising background. For example, the 0.5-mm detector used to obtain the spectrum of Fig. 2 could be used for protons of energies from 2.5 to 15 MeV, since 15-MeV protons lose 2.5 MeV in this detector and thus are separated from background. For deuterons, this same detector could be used over the range of 2.5 to 25 MeV. Often two detectors were used in tandem, but not in time coincidence. A front, relatively thin detector, would be used to detect deuterons, and a back, thick detector, would detect the protons.

Every 10 min, during each He^3 data run, the target was changed for 2 min to the H^2 gas cell. The magnet setting was adjusted to focus H^2 photoprotons corresponding to the gamma-ray energy that produced the photodeuterons in the He^3 run. The H^2 pulse-height spectrum was accumulated in a separate 200-channel memory block of the analyzer. By this method the spectrum of gamma rays was monitored. The integrated current from an argon-methane gas-filled ionization chamber was used to normalize the photon beam intensity between the He^3 and H^2 runs. The reliability of the ionization chamber as a monitor for the gamma-ray intensity was established by a comparison of a number of runs using the deuterium-gas cell target.

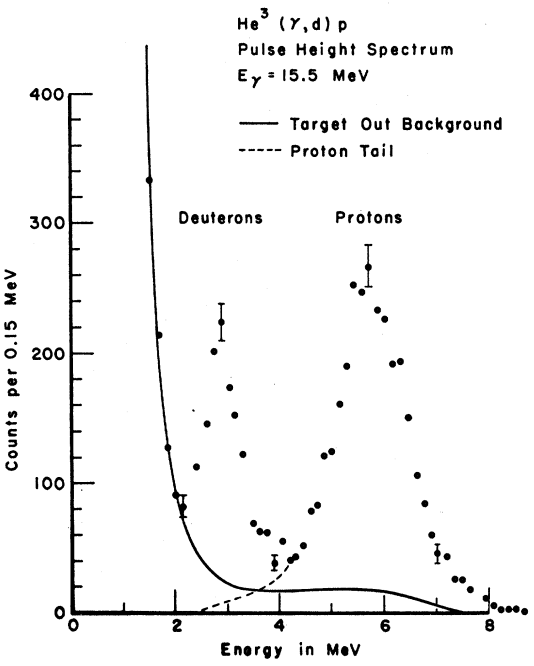

FIG. 2. Pulse-height spectrum from a 0.5-mm detector is shown for one magnet setting. The deuteron energy corresponds to 15.5 MeV gamma-ray energy when corrections are applied for loss in target gas and foil.

III. DATA ANALYSIS

A. Two-Body Breakup: $He^3(\gamma,d)p$

The total number of deuteron counts in a spectrum peak for each run was determined by subtracting the background obtained in a run with an evacuated target cell and the quadrupole magnet at a similar field setting. The largest error was in determining the separation of the proton and deuteron counts in the overlapping tails of the two peaks. The shape of the tails was determined in two ways. First, a H^2 run at the same magnet setting would give the approximate shape of the proton peak. Second, the expected shape of the spectrum peak could be determined more exactly by multiplying together the following three factors: the bremsstrahlung spectrum, an assumed He^3 cross section, and the magnet transmission curve. The transmission curve is the solid angle seen by the detector as a function of E/E_0, where E is the actual proton energy and E_0 is the proton energy corresponding to optimal focussing. This curve is independent of E_0, and was determined in a subsidiary measurement.[2] The uncertainty in the shape of the tails contributed about 5% error. Most of the remaining quoted errors were due to statistics either of foreground or background or both, depending on the detector and the deuteron energy.

The midpoint energy assigned to the deuteron peak observed in each run was determined by the magnet-field setting, with corrections for the shift in the midpoint of the peak due to the variation with proton energy of the photodisintegration cross section and to the bremsstrahlung spectrum shape. The quadrupole magnet was calibrated by means of the 5.30-MeV alphas from Po^{210} and 9.55-MeV photoprotons from O^{16}. The formula

[2] J. S. O'Connell, J. R. Stewart, and R. C. Morrison, Nucl. Instr. Methods **30**, 229 (1964).

used to evaluate the cross sections was the following:

$$\left.\frac{d\sigma}{d\Omega}\right|_{90°\text{lab}}(\text{He}^3)=\frac{4}{3}\frac{N_d(\text{He}^3)}{P(\text{He}^3)I(\text{He}^3)E_d(\text{He}^3)}\times\frac{P(\text{H}^2)I(\text{H}^2)E_p(\text{H}^2)}{N_p(\text{H}^2)}\left.\frac{d\sigma}{d\Omega}\right|_{90°\text{lab}}(\text{H}^2),$$

where $N_d(\text{He}^3)$ is the total number of deuteron counts from He^3 contained in a peak; $N_p(\text{H}^2)$ is the total number of proton counts from H^2 contained in a peak produced by the same gamma energy; $P(\text{He}^3)$ and $P(\text{H}^2)$ are the gas pressures measured to $\pm 0.5\%$ with mercury manometers; $I(\text{He}^2)$ and $I(\text{H}^2)$ are the respective cumulative monitor-chamber readings.

$E_d(\text{He}^3)$ and $E_p(\text{H}^2)$ are the respective energies of the particles which are observed by the magnet. These factors are included to normalize the number of particles to counts per megaelectron volt. This results from the fact that the area under a transmission curve is proportional to the particle energy.

$d\sigma/d\Omega|_{90°\text{lab}}(\text{H}^2)$ is the deSwart and Marshak[3] theoretical cross section for H^2 transformed to 90° in the lab.

The quantity $\frac{4}{3}$ is a normalizing factor containing a factor of 2 because H^2 is diatomic and He^3 monatomic, and a kinematic factor of $\frac{2}{3}$ arising from the fact that $\Delta E_\gamma/\Delta E_p=2$ for H^2 and $\Delta E_\gamma/\Delta E_d=3$ for He^3.

The results of a number of runs are presented in Table I and Fig. 3. The photon energy widths correspond to the full width at half-maximum of the deuteron peak. This width contains about 70% of the counts in each peak. The actual midpoint energies were all known to better than $\pm 2\%$. In the center-of-mass system the angle of the deuteron with respect to the gamma varied from about 95° at 10 MeV to 98° at 46 MeV.

The quoted errors include statistical as well as estimates of systematic errors but do not include any estimate of the error in the deSwart and Marshak H^2 cross section. This theory was used since it fits the experimental H^2 cross-section data reasonably well in the region of interest for this experiment. The estimate of possible systematic error from this source is $\pm 10\%$.

TABLE I. $\text{He}^3(\gamma,d)p$ differential cross section at 90° lab.

E_γ (MeV)	$d\sigma/d\Omega$ (μb/sr)
8.9±0.4	83±10
10.3±0.5	90±7
12.6±0.8	87±10
13.6±1.0	90±7
14.4±1.2	85±5
15.6±1.3	74±4
16.8±1.5	70±6
18.8±1.8	64±5
20.0±2.0	59±4
23.0±2.5	50±4
27.7±3.3	32±3
34.3±4.3	19±4
41.0±5.5	18±8
46.1±6.1	10±7

[3] J. J. deSwart and R. E. Marshak, Physica **25**, 1001 (1959).

B. Three-Body Breakup: $\text{He}^3(\gamma,2p)n$

The experimental arrangement together with the reaction kinematics require that the number of proton counts from the two-body breakup reaction at a given photon energy equal the number of deuteron counts. Thus, any "excess" protons contained in a proton peak must be from three-body breakup. Because of energy-loss effects in the gas target, corrections to the observed numbers of deuteron counts and proton counts had to be made to make them correspond to the same photon energy. Figure 4 shows a plot of the number of three-body breakup protons per atom per megaelectron volt of proton energy per monitor reading. The data were all taken with a bremsstrahlung end point of 40±3 MeV.

IV. COMPARISON WITH OTHER EXPERIMENTS

In this section we summarize the results of other photodisintegration experiments on H^3 and He^3. The five experiments at 90° (in the lab system) are compared with each other in Fig. 5(a) and discussed in Sec. A. The results of the four total-cross-section measurements (including two on H^3) are shown in Fig. 5 (b) and discussed in Sec. B. In Sec. C, the differential cross sections are compared with the total cross sections.

A. 90° Differential-Cross-Section Experiments

There have been one low-energy capture experiment and four medium-energy photodisintegration experi-

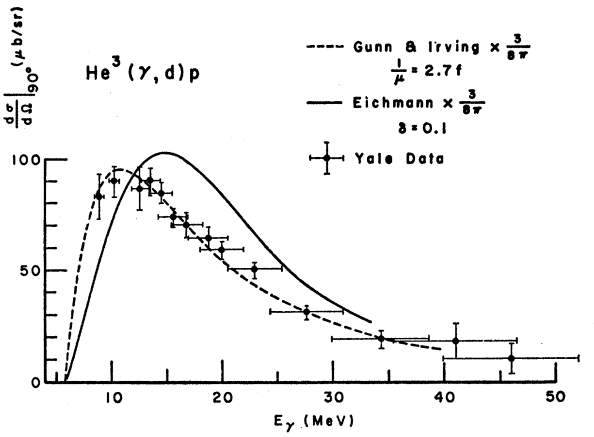

FIG. 3. Final experimental $\text{He}^2(\gamma,d)p$ data is compared with two theoretical predictions. The vertical error bars are combined from statistical errors and estimates of systematic errors for each point. The horizontal error bars are the full width at half-maximum for each point. This width includes about 70% of the data used for each point. The dashed curve is from Gunn and Irving (Ref. 18) with $1/\mu=2.7$ F assuming a pure $\sin^2\theta$ distribution, $(d\sigma/d\Omega|_{90°}=\sigma_{\text{total}}3/8\pi)$. The solid curve is from Eichmann (Ref. 20) with mixing parameter $\delta=0.1$, and again the total cross section is multiplied by $3/8\pi$ to compare with the data.

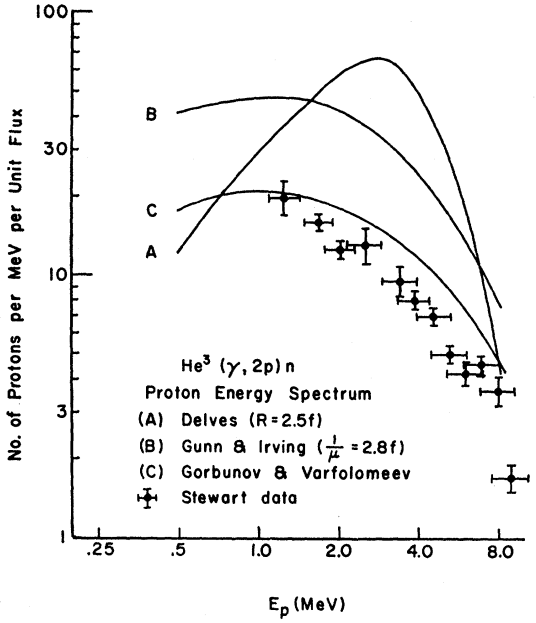

FIG. 4. The proton spectrum from three-body breakup produced by 40-MeV bremsstrahlung. The three curves shown are calculations made with different three-body breakup cross sections: theories by Delves (Ref. 21) and by Gunn and Irving (Ref. 18); and an experiment by Gorbunov and Varfolomeev (Ref. 13).

ments on He^3 at 90°. Of the four medium-energy experiments, three (Berman *et al.*[4]; Finckh *et al.*[5]; and the present work) agree within experimental error and one (Becchi *et al.*[6]) is roughly a factor of two larger.

Griffiths *et al.*[7–9] have measured the cross section and angular distribution of capture gamma rays for the reaction $D(p,\gamma)He^3$ from very low center-of-mass excitation energies up to 1.2 MeV. Their results for the 90° differential capture cross section have been transformed to the photodisintegration cross section using the detailed balance formula. The angular distribution was found to be very nearly $\sin^2\theta$, showing the reaction to be predominantly dipole. Wilkinson[10] has shown by a measurement of the gamma-ray polarization that at low energies the capture reaction, hence the photodisintegration, is predominantly *electric* dipole.

Berman *et al.*[4] measured the He^3 two-body breakup at 90° in the lab from 8.5 to 21.5 MeV by detecting proton-deuteron coincidences in CsI(Tl) scintillators. A 22-MeV betatron was the source of the gamma rays.

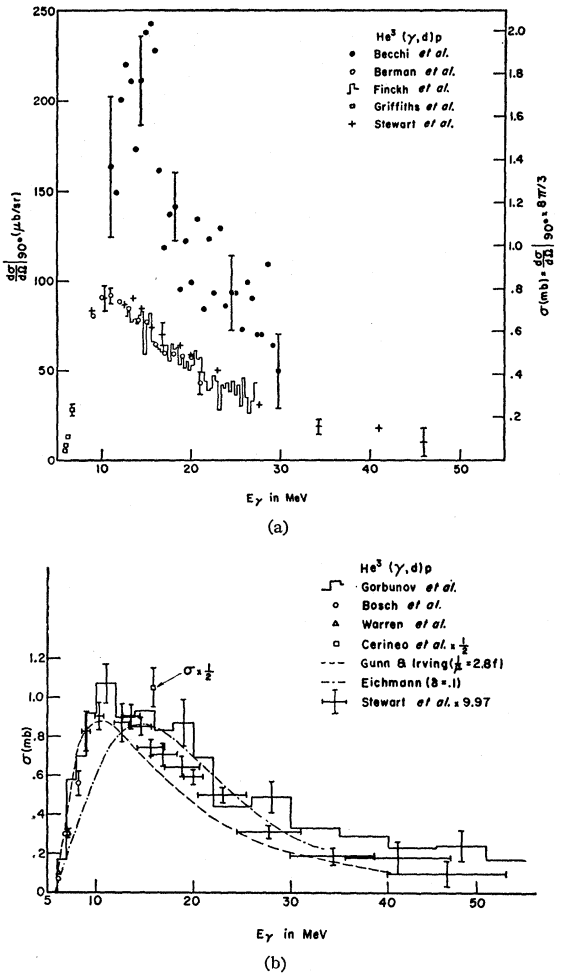

FIG. 5. (a) Comparison of experimental 90° differential two-body breakup cross sections. The right-hand ordinate shows the total cross section assuming a $\sin^2\theta$ angular distribution. Shown with some representative error bars are two-body photodisintegration data from Becchi *et al.* (Ref. 6) (data as published is divided by $3/8\pi$ to compare with the rest of 90° data), Berman *et al.* (Ref. 4), Finckh *et al.* (Ref. 5), and the present experiment as well as low-energy capture data from Griffiths *et al.* (Refs. 7–9) (transformed by detailed balance). (b) Comparison of experimental total two-body breakup cross sections. Shown with some representative error bars are He^3 photodisintegration data from Bösch *et al.* (Ref. 12) and $D(n,\gamma)T$ capture from Cerineo *et al.* (Ref. 14) both corrected for different thresholds of H^3 and He^3, and He^3 photodisintegration data from Gorbunov *et al.* (Ref. 13) and Warren *et al.* (Ref. 11). The data of the present experiment are multiplied by a factor of 9.97 in accordance with the angular distribution of Gorbunov *et al.* (Ref. 13). The curves are theoretical predictions of Gunn and Irving (Ref. 18), $\mu^{-1}=2.8$ F, and Eichmann (Ref. 20).

Their 90° differential cross section is shown in Fig. 5(a). They also have some data on the three-body breakup from proton-proton coincidences at 180° to each other and 90° to the photon beam. With some assumptions about the angular distribution they find $d\sigma$ (3-body) $=3.3\ d\sigma$ (2-body).

Finckh *et al.*[5] also measured the 90° differential cross section for the two-body breakup over the energy

[4] B. L. Berman, L. J. Koester, and J. H. Smith, Phys. Rev. **133**, B117 (1964).
[5] E. Finckh, R. Kosiek, K. H. Lindenberger, U. Meyer-Berkhout, N. Nücker, and K. Schlüpmann, Phys. Letters **7**, 271 (1963).
[6] C. Becchi, G. E. Manuzio, L. Meneghetti, and S. Vitale, Phys. Letters **8**, 322 (1964).
[7] G. M. Griffiths, E. A. Larson, and L. P. Robertson, Can. J. Phys. **40**, 402 (1962).
[8] G. M. Griffiths, M. Lal, and C. D. Scarfe, Can. J. Phys. **41**, 724 (1963).
[9] G. M. Griffiths and J. B. Warren, Proc. Phys. Soc. (London) **A68**, 781 (1955).
[10] D. H. Wilkinson, Phil. Mag. **43**, 659 (1952).

range of 12.5 to 27.5 MeV, using nearly the same technique as Berman *et al.*

Becchi *et al.*[6] measured the He^3 two-body cross section at 90° from 10 to 30 MeV with a coincidence technique and with a mass-discriminating counter telescope. They claim fine structure in the cross section and also find a very large low-energy cross section. Their data is published as a total two-body cross section, although only a 90° measurement was made. Their data is shown divided by $8\pi/3$ in Fig. 5(a) to convert it back to a differential cross section (i.e., assuming a $\sin^2\theta$ distribution).

B. Total Two-Body Cross Sections

The total cross section has been measured by one neutron-capture experiment, two low-energy photodisintegration experiments and two medium-energy photodisintegration experiments. The low-energy data of Warren *et al.*[11] and Bösch *et al.*[12] agree well with each other and with the low-energy data from Gorbunov *et al.*[13] The neutron capture result of Cerineo *et al.*[14] is a factor of 2 larger than those of Gorbunov. The data from Cranberg[15] is not included since he was unable to distinguish protons from deuterons.

Warren *et al.*[11] have measured the two-body breakup cross section at gamma-ray energies of 6.14, 6.97, and 7.08 MeV by using a gridded ionization chamber and the gamma rays from the reaction, $F^{19}(p,\alpha\gamma)$. These results are in good agreement with those of Griffiths *et al.* (assuming a $\sin^2\theta$ distribution).

Bösch *et al.*[12] using the monoenergetic gamma rays from (n,γ) reactions, measured three points on the H^3 $(\gamma,n)d$ total-cross-section curve at low energies.

Cerineo *et al.*[14] measured the capture cross section of 14.4-MeV neutrons by deuterons. This total-capture cross section, converted by the detailed balance formula, yields a photodisintegration total cross section of 2.1 ± 0.4 mb at 15.86 MeV.

The most complete photodisintegration experiment to date is that of Gorbunov and Varfolomeev.[13,16] Using 170-MeV bremsstrahlung they measured both the two-body and three-body photodisintegration cross sections with a cloud chamber filled with He^3 and operated in a magnetic field. The final results[13] agree quite well with those of the present experiment and Refs. 4 and 5. Gorbunov and Varfolomeev find that the angular distribution for two-body breakup, averaged over the whole energy range, is given by

$$0.03+\sin^2\theta(1+0.66\cos\theta+0.46\cos^2\theta)$$

instead of a pure dipole $\sin^2\theta$ as was previously thought.

C. Comparison of Differential and Total Cross Sections

To compare differential and total two-body cross sections a factor, $(\int W(\theta)d\Omega)/W(\theta)$ [where $W(\theta)$ is the differential cross section], which in general depends on gamma-ray energy, must be calculated. For a pure dipole transition, this factor is $(8\pi/3)/\sin^2\theta$, independent of energy. This conversion is shown in the right-hand ordinate of Fig. 5(a).

If we use the angular distribution of Ref. 13, this factor becomes $(\int W(\theta)d\Omega)/W(96°)=9.97$. An average center-of-mass angle of 96° is used for our data. Our differential cross-section data converted by this factor are shown in Fig. 5(b). The data are no longer well fitted by a Gunn and Irving two-body cross section of any radius parameter (as would be expected since this theory did not consider $E2$ transitions). The Eichmann total two-body cross section is now a better fit to our data. This conversion procedure is somewhat dubious since the differential-to-total cross-section conversion factor would be expected to be energy-dependent.

V. COMPARISON WITH THEORY

A. Theories of the Photodisintegration of He^3 and H^3

There have been five calculations[17–21] of the photodisintegration cross section of the three-nucleon system, He^3 and H^3. Three of these calculations[17–19] are quite similar, differing only in the choice of the form of the ground-state wave function. He^3 and H^3 are treated alike except that a Coulomb-barrier correction is applied to the final cross section for He^3 at low energies (from 0 to 2 MeV above threshold).

Verde[17] and Gunn and Irving[18] calculated the two- and three-body cross section for H^3 using a Gaussian wave function for the ground state:

$$\Psi=\text{const.}\exp[-\mu\sum_{i<j}r_{ij}^2].$$

This form is readily integrable; however, the asymptotic form falls off faster than the correct solution. Since the photonuclear matrix element is sensitive to the tail of the ground-state wave function, especially at low energies, this function is not expected to give correct cross section results.

For space-symmetric ground-state wave functions, like the Gaussian, Verde has shown that the magnetic-

[11] J. B. Warren, K. L. Erdman, L. P. Robertson, P. A. Axen, and J. R. MacDonald, Phys. Rev. **132**, 1691 (1963).
[12] R. Bösch, J. Lang, R. Müller, and W. Wölfli, Phys. Letters **8**, 120 (1964).
[13] A. N. Gorbunov and A. T. Varfolomeev, Phys. Letters **11**, 137 (1964).
[14] M. Cerineo, K. Ilakovac, I. Slaus, and P. Tomas, Phys. Rev. **124**, 1947 (1961).
[15] L. Cranberg, Bull. Am. Phys. Soc. **3**, 173 (1958); and (private communication).
[16] A. N. Gorbunov and A. T. Varfolomeev, Phys. Letters **5**, 149 (1963).
[17] M. Verde, Helv. Phys. Acta **23**, 453 (1950).
[18] J. C. Gunn and J. Irving, Phil. Mag. **42**, 1353 (1951).
[19] C. Rossetti, Nuovo Cimento **14**, 1171 (1959).
[20] U. Eichmann, Z. Physik **175**, 115 (1963).
[21] L. M. Delves, Nucl. Phys. **29**, 268 (1962).

dipole transition for the two-body breakup is forbidden on the basis of symmetry arguments. The electric-dipole transition should then dominate at low to medium energies. The final-state wave function for two-body breakup was taken by both Verde, and Gunn and Irving as the product of the $l=1$ part of a plane wave for the outgoing neutron from H^3 (or proton from He^3) and a Gaussian function $[\exp(-\mu_D r_{12}^2)]$ for the remaining deuteron. This plane-wave assumption would seem physically plausible since P-wave nucleon-deuteron forces are known to be relatively weak. In three-body breakup, two plane waves were used. The magnetic dipole transition is not forbidden for the three-body breakup, and Verde has given an expression for the cross section.

Gunn and Irving have also evaluated the two- and three-body electric dipole photodisintegration cross sections, using ground-state wave functions having a more suitable asymptotic behavior. There is a class of wave functions called Irving[22] functions that have the form

$$\Psi=\text{const.}\{\exp[-\mu(\sum_{i<j} r_{ij}^2)^{1/2}]/(\sum_{i<j} r_{ij}^2)^n\}.$$

Gunn and Irving evaluated σ(2-body) and σ(3-body) for $n=\frac{1}{2}$. Rossetti[19] evaluated σ(2-body) for $n=0$. The $l=1$ part of a plane wave was used for the proton and $\exp[-\mu_D r_{23}]/r_{23}$ for the deuteron final state in both cases. The three results for σ(2-body): Gaussian, Irving $n=0$, and Irving $n=\frac{1}{2}$, are shown in Fig. 6 for reasonable values of the radius parameters. Radius parameters for the Gaussian and Irving ($n=0$) ground-state wave functions have been evaluated by Schiff[23] by best fits to the He^3 and H^3 electron-scattering data. These values of the parameters also give the correct Coulomb energy for He^3.

Eichmann[20] has calculated the two-body breakup including the effects of (1) nonsymmetric components in the ground-state wave function; (2) quadrupole contributions to the transition matrix element; and (3) final-state interactions between the outgoing particle and the deuteron. Eichmann took the symmetric part of the three-body ground state as a sum of two Gaussian terms. The parameters were chosen from a variational calculation giving approximately the binding and Coulomb energies of H^3 and He^3. Additional terms of mixed symmetry were added with an amplitude ratio of $\delta=0.1$.

The electromagnetic transition operator included the electric quadrupole as well as the electric dipole terms. The final-state wave function was taken as the product of the wave functions of the deuteron ground state (the sum of two Gaussians) and the outgoing protons. This last was treated two ways: first, as the $l=1$ part of a plane wave; and second, by calculating the phase shift due to the final-state interaction between the neutron (for H^3) and the deuteron.

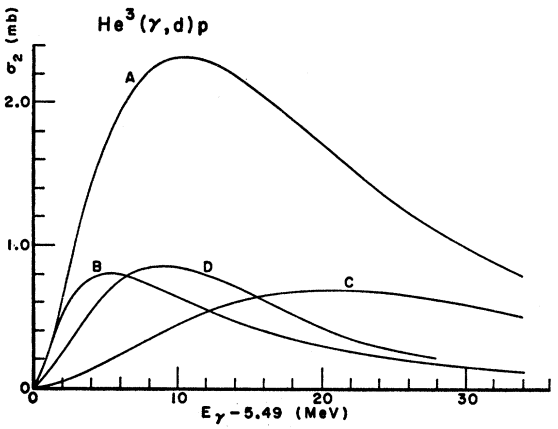

FIG. 6. Various theoretical predictions for $He^3(\gamma,d)p$ are compared. The ground-state radius parameters for each theory are chosen to give reasonable agreement with binding energy and Coulomb-energy calculations and, in the case of curves A and C, fits to elastic electron-scattering data (Ref. 23).

Curve A: Irving (Refs. 19, 23): $n=0$, $\alpha=0.2317$ F^{-1}, $\beta=0.8980$ F^{-1}.
Curve B: Irving (Ref. 18): $n=\frac{1}{2}$, $\mu_T=0.371$ F^{-1}.
Curve C: Gaussian (Refs. 18, 23): $\mu_T=0.2716$ F^{-1}, $\mu_D=0.3042$ F^{-1}.
Curve D: Eichmann (Ref. 20): $c_1=0.3$ F^{-2}, $c_2=0.07$ F^{-2}.

The resulting cross sections show: (1) the nonsymmetric terms in the ground-state shift the peak to a lower gamma energy but leave the integrated cross section to 30 MeV relatively unchanged; (2) the inclusion of the quadrupole interaction term has a dramatic effect for He^3 (but not for H^3) in the differential cross section and the angular distribution; and (3) the inclusion of the final-state interaction is found to increase the total cross section, at the peak, by about 25%.

Figure 3 shows the Eichmann 90° result for $\delta=0.1$, with quadrupole transitions, but no final-state interaction. This curve was generated by dividing the total cross section curve by $8\pi/3$. This is not strictly correct since the angular distribution is not pure $\sin^2\theta$ and changes with energy.

B. Discussion of Two-Body Results

The data agree better with the Gunn and Irving ($n=\frac{1}{2}$) and the Eichmann calculations as compared with the Gaussian and the Irving ($n=0$) calculations. Of the first two, the Gunn and Irving gives the best fit, but we adjusted the radius parameter for the best fit to the data, while the Eichmann radius parameters were fixed from a binding-energy calculation.

C. Discussion of Three-Body Results

One can take the Gunn and Irving three-body cross section [Fig. 7(a)] (based on the $n=\frac{1}{2}$ wave function) together with the proton spectrum expected from the

[22] J. Irving, Phil. Mag. **42**, 338 (1951).
[23] L. Schiff, Phys. Rev. **133**, B802 (1964).

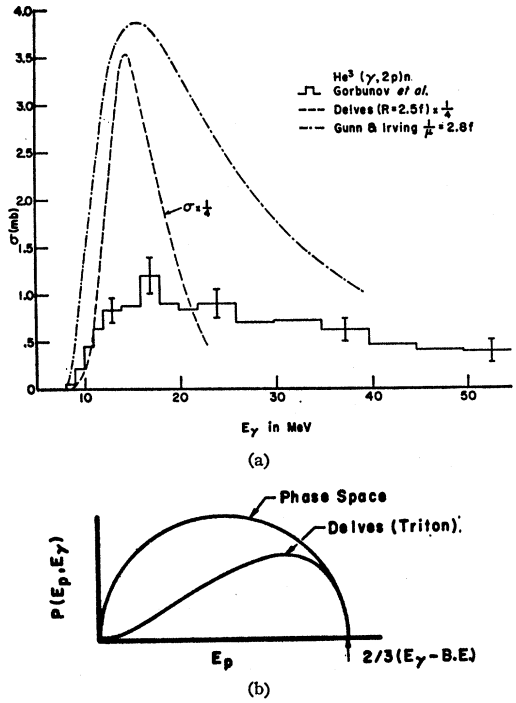

FIG. 7. (a) Three-body breakup cross sections. The dashed curve is from Delves (Ref. 21) ($R=2.5$ F) divided by a factor of 4; the dot-dash curve is from Gunn and Irving (Ref. 18) ($\mu^{-1}=2.8$ F); and the histogram is the experimental cross section of Gorbunov and Varfolomeev (Ref. 13). (b) Proton energy distribution for two different assumptions about the final-state interaction.

breakup at one photon energy, to predict the expected total proton-energy spectrum from a bremsstrahlung experiment. In the Gunn and Irving case, where there are no final-state interactions, the proton spectrum from the gamma ray of energy E_γ is given by the phase-space expression [see Fig. 7(b)]:

$$P(E_p,E_A)=(18/\pi E_A^2)(\tfrac{2}{3}E_AE_p-E_p^2)^{1/2},$$

where, $E_A=E_\gamma+Q$, and $Q=-7.72$ MeV. The normalization is

$$\int_0^{2/3E_A} PdE_p=1.$$

The folding of the three-body cross section, $d\sigma_3(E_\gamma)$, the proton energy distribution, $P(E_p,E_\gamma)$, and the bremsstrahlung spectrum, $N_\gamma(E_\gamma)$, to predict the observed energy spectrum is given by

$$N_{3p}(E_p)=\eta\Omega\int_0^{40}N_\gamma(E_\gamma)\frac{d\sigma_3(E_\gamma)}{d\Omega}\bigg|_{\pi/2}P(E_p,E_\gamma)dE_\gamma,$$

where η is the effective number of He^3 nuclei in the beam and Ω is the solid angle. The bremsstrahlung spectrum as measured by the $H^2(\gamma,p)$ reaction, was found to be nearly E_γ^{-1} over the energy region of interest. The predicted proton spectrum is shown as curve B in Fig. 4.

The Gunn and Irving prediction is seen to give a shape in agreement with the data, but a factor of 2 too large in magnitude. The Gunn and Irving total σ(3-body) was divided by 4π (assuming an isotropic proton angular distribution) to compare with experiment. This is not correct; the actual angular distribution lies somewhere between isotropic and $\sin^2\theta$ since the three-body breakup involves both P- and S-wave particles. This will make the disagreement with experiment even larger.

One might expect that the Gunn and Irving three-body cross-section calculation is incorrect because of the plane-wave assumption for the S-wave particles. A better three-body cross section would result if the known nucleon-nucleon S-wave phase shift were included in the final-state wave functions.

Delves[21] has calculated the three-body cross section for H^3. The cross section is shown in Fig. 7(a). (Notice that the cross section is shown divided by a factor of 4.) Final-state interactions for H^3, according to Delves, produce a proton-energy distribution as shown in Fig. 7(b). Assuming that this same distribution applies to He^3 protons, the folding integral yields the curve A shown in Fig. 4. Agreement is not good in shape or magnitude.

We have also taken the three-body cross sections as measured by Gorbunov and Varfolomeev[13] [see Fig. 7(a)] and folded it with the phase-space distribution. This curve, shown in Fig. 4, is systematically larger than the data but gives the best agreement of the three calculations.

The three-body prediction for a Gaussian ground-state wave function was not made since the two-body results were in such poor agreement with experiment.

VI. SUM-RULE CALCULATIONS

In this section, we discuss various theoretical calculations of the electric-dipole sum rules for the total photodisintegration cross section of He^3 and H^3, viz:

integrated cross section:

$$\sigma_{\rm int}=\int_0^\infty\sigma_{\rm abs}(E_\gamma)dE_\gamma,$$

bremsstrahlung-weighted integrated cross section:

$$\sigma_b=\int_0^\infty\frac{\sigma_{\rm abs}(E_\gamma)}{E_\gamma}dE_\gamma,$$

where $\sigma_{\rm abs}$ is the total absorption cross section. We compare the results of these calculations with the available experimental data.

A. The Integrated Cross Section, $\sigma_{\rm int}$

Two approaches to calculating $\sigma_{\rm int}$ have been made. One approach is to extend the Thomas-Reiche-Kuhn

sum rule,

$$\sigma_{\text{int}}=\frac{2\pi^2he^2}{mc}\frac{NZ}{A}=60\frac{NZ}{A}\text{ MeV mb},$$

to include exchange forces. A second approach is the use of the dispersion relations.

In the first approach, Levinger and Rustgi[24] and Douglas[25] have given an expression for σ_{int} that depends on both the assumed two-body nuclear potential and the ground-state wave function of the nucleus in question. Rustgi[26] has evaluated σ_{int} for He^3 and H^3 using a two-body spin-dependent Yukawa potential with Heisenberg (space and spin exchange) and Majorana (space exchange) forces. Rustgi uses an Irving[22] type wave function with $n=0$. The result evaluated for $\mu=0.92$ F^{-1} is

$$\sigma_{\text{int}}=40[1+0.55(x+\tfrac{1}{2}y)]\text{ MeV mb},$$

where x is the fraction of Majorana exchange force and y is the fraction of Heisenberg exchange. A commonly used set of values for x and y, the Rosenfeld exchange mixture $x+\frac{1}{2}y=0.80$, gives $\sigma_{\text{int}}=58$ MeV-mb.

Mathur, Mukherjee, and Rustgi[27] have redone this calculation using two-body spin-dependent forces for exponential type with *hard core*. They use a Kikuta[28] ground-state wave function whose radius constants are adjusted to give the correct binding energy of H^3 and Coulomb energy of He^3. The hard-core radius is taken as 0.4 F. The result is

$$\sigma_{\text{int}}=40[1+0.72(x+\tfrac{1}{2}y)]\text{ MeV mb},$$

that is, the coefficient of the exchange mixture is 0.72 instead of 0.55 for a non-hard-core wave function. Thus, for the Rosenfeld mixture, $\sigma_{\text{int}}=63$ MeV mb.

Davey and Valk[29] evaluated σ_{int} using a two-body potential which included both a repulsive core and a tensor-force component. The potential parameters are chosen to give a reasonable fit to the static properties of H^2, H^3, He^3, and He^4. The ground-state wave function is calculated by perturbation methods from S-state orbitals of a single-particle harmonic oscillator Hamiltonian. These authors find that the value of $\sigma_{\text{int}}=63$ MeV-mb can be obtained either with a repulsive core potential or by a tensor component in the two-body potential. The effect of repulsive core and tensor forces is more important in σ_b, as we shall see later.

A second approach to evaluating σ_{int} is to use the dispersion relation. This method as applied by Gell-Mann, Goldberger, and Thirring[30] (GGT) has the following advantages: (1) all multipole transitions are included, not just the electric dipole; (2) no assumptions are made about the nuclear forces or wave functions; and (3) the upper limit of integration in the sum rule is clearly specified as the threshold for meson production ($\sim$150 MeV), whereas the Levinger and Rustgi limit is taken as infinity, but loses its applicability above meson threshold. The disadvantage of the GGT sum rules is that the high-energy cross sections needed to evaluate the term which is added to the Thomas-Reiche-Kuhn value are poorly known. The dispersion result is

$$\sigma_{\text{int}}=\int_0^{\mu}\sigma_{\text{abs}}dE_\gamma=60\frac{NZ}{A}+\int_{\mu}^{\infty}(Z\sigma_p+N\sigma_n-\sigma_A)dE_\gamma,$$

where μ is the meson photoproduction threshold and σ_p, σ_n, and σ_A are the total photon absorption cross sections for the proton, neutron, and for the nucleus under discussion; these are usually taken as the meson production cross sections. GGT evaluated the integral on the right-hand side using experimental data to give $\sigma_{\text{int}}=60(NZ/A)[1+0.1(A^2/NZ)]$ by assuming that the integral was proportional to A. For the three-nucleon system, this yields $\sigma_{\text{int}}=58$ MeV-mb which is in agreement with the other three explicit calculations of σ_{int}. The value of the coefficient of A^2/NZ can also be obtained by using the experimental sum-rule data for H^2 and He^4 and taking the average for $A=3$. The coefficient for H^2 is 0.075, while for He^4 it is 0.142 giving an average of 0.108 in agreement with the value used above.

Danos[31] has pointed out that the apparent constancy of high-energy cross sections causes the integral over the cross-section difference to become divergent, so that one more subtraction must be made leaving the forward scattering amplitude difference at infinite energy as a remainder.

B. The Bremsstrahlung-Weighted Integrated Cross Section σ_b

The σ_b sum rule has been evaluated only by the Levinger and Bethe[32] method.

$$\sigma_b=\frac{4\pi^2}{3}\left(\frac{e^2}{\hbar c}\right)\int\psi_0[\textstyle\sum_p(\mathbf{r}_p-\mathbf{R})]^2\psi_0 d\mathbf{r},$$

where $\mathbf{r}_p$ are the proton coordinates, and $\mathbf{R}$ is the center-of-mass coordinate. Foldy[33] has shown, for nuclei in which the ground-state wave function ψ_0 is symmetric in space coordinates of all the nucleons, that

[24] M. L. Rustgi and J. S. Levinger, Phys. Rev. **106**, 530 (1957).
[25] Quoted by D. Dixon, *Nuclear Forces and the Few Nucleon Problem*, edited by T. C. Griffith and E. A. Power (Pergamon Press Inc., New York, 1960), Vol. I, p. 307.
[26] M. L. Rustgi, Phys. Rev. **106**, 1256 (1957).
[27] V. S. Mathur, S. N. Mukherjee, and M. L. Rustgi, Phys. Rev. **127**, 1663 (1962). (Note that Ref. 29 corrects the value of σ_b given in this paper.)
[28] T. Kikuta, M. Morita, and M. Yamada, Progr. Theoret. Phys. (Kyoto) **15**, 222 (1956).
[29] P. O. Davey and H. S. Valk, Phys. Letters **7**, 155 (1963).
[30] M. Gell-Mann, M. L. Goldberger, and W. E. Thirring, Phys. Rev. **95**, 1612 (1954).
[31] M. Danos, Bull. Am. Phys. Soc. **6**, 432 (1961).
[32] J. S. Levinger and H. A. Bethe, Phys. Rev. **78**, 115 (1950).
[33] L. L. Foldy, Phys. Rev. **107**, 1303 (1957).

σ_b for electric dipole absorption is simply related to the mean-square radius of the matter distribution (i.e., nucleon centers distribution). This relationship is independent of the existence of correlations between the motions of the nucleons. The relationship is

$$\sigma_b=\frac{4\pi^2}{3}\left(\frac{e^2}{\hbar c}\right)\frac{ZN}{A-1}\langle r^2\rangle_{\text{matter}}=0.96\frac{ZN}{A-1}\langle r^2\rangle_m.$$

The mean-square matter radius $\langle r^2\rangle_m$ can be related to the mean-square charge radius $\langle r^2\rangle_c$, as measured by elastic electron scattering, by unfolding the mean-square charge radius of the proton. This can be done to a good approximation by taking

$$\langle r^2\rangle_m=\langle r^2\rangle_c-\langle r^2\rangle_c^{\text{proton}},$$

with $\langle r^2\rangle_c^{\frac{1}{2}\text{proton}}=0.805$ F.[34] Foldy[33] shows that this procedure gives good agreement between the experimental photonuclear σ_b and electron scattering measurement of $\langle r^2\rangle_c$ for H^2 and He^4. Recent measurements by Collard *et al.*[35,36] yield charge radii

$$He^3:\ \langle r^2\rangle_c^{1/2}=1.97\pm0.10\text{ F},$$
$$H^3:\ \langle r^2\rangle_c^{1/2}=1.68\pm0.16\text{ F}.$$

(Note that the relative error between these two values is smaller than the absolute error because the measurements were done concurrently.) The fact that these two radii are not the same implies that the proton wave functions are not the same for the two nuclei.

Schiff[36] analyzes these data by taking one spatial distribution for the *like* pair of nucleons (protons in He^3 and neutrons in H^3) and another distribution for the *odd* particles. The ground-state wave function then consists of a space symmetric term (S) and a term of mixed spatial symmetry (S'). Although the amplitude of S' is only a few percent of S, the cross term $S\cdot S'$ makes a sizeable difference in the charge radii of He^3 and H^3.

Srivastava[37] taking a fully symmetric ground-state wave function $\exp[-\frac{1}{2}k(r_{12}+r_{23}+r_{13})]$ finds that $k=0.74$ F^{-1} gives a good value of the Coulomb energy of He^3. He then calculates the matter form factor F_m and uses the Collard *et al.* data to give the experimental value by the following formula:

$$F_m(q^2)=\frac{2F_c(\text{He}^3)+F_c(\text{H}^3)}{3[F_c(p)+F_c(n)]}.$$

A fairly good fit is found. The Foldy formula then gives $\sigma_b=3.0$ mb (since the above value of k gives $\langle r^2\rangle_m^{1/2}=1.76$ F).

Davey and Valk[38] evaluate $\langle r_{pn}^2\rangle^{1/2}$ using a Gaussian wave function containing a 3.5% of S'. They find $\langle r_{pn}^2\rangle^{1/2}=2.16$ F, giving $\sigma_b=1.99$ mb. To this value, the S term contributed 2.17 mb and the S' term -0.18 mb. Radha and Meister[39] from analysis of the rate of neutron capture by deuterons have indicated an upper limit of 2% S' state. This value would increase the Davey and Valk result only slightly. The disagreement between the Srivastava, and the Davey and Valk values of σ_b, both derived from the Collard data, is due to the different types of wave functions used (exponential versus Gaussian). Since the Gaussian wave function does not give agreement with the two-body photodisintegration data, the exponential wave function value of $\sigma_b=3.0$ mb should probably be trusted more.

There are three calculations of σ_b using the explicit ground-state wave functions mentioned earlier in calculations of σ_{int}. Rustgi, with no hard core or tensor forces, gets $\sigma_b=1.32$ mb; Mathur *et al.* with a hard-core potential get $\sigma_b=2.85$ mb; Davey and Valk, with a repulsive core and/or tensor forces, get $\sigma_b=2.36$ mb. As can be seen, σ_b is sensitive to repulsive core and tensor forces, but not to exchange mixtures, while for σ_{int}, the reverse is true.

C. σ_{int} and σ_b from Specific Photonuclear Calculations

Shown in Table II are values of σ_{int} and σ_b we have found by analytical or numerical integration of various theories for $\sigma^{2\text{-body}}$ and $\sigma^{3\text{-body}}$. It is apparent that the values of σ^{total} are too large when compared to the values in Table III. This discrepancy between theories can be attributed to the fact that in calculating the photodisintegration cross sections the final-state plane waves used are not eigenfunctions of the Hamiltonian that produced the ground state. In the two-body breakup a Serber mixture of exchange forces giving zero interaction in the $l=1$ state would make a plane wave an eigenfunction; however, in the three-body breakup, since two of the particles are in a relative S state, the plane wave is a bad approximation.

Thus we would expect that the Irving $n=\frac{1}{2}$ ground-state wave function and plane-wave final states (the Gunn and Irving calculation) would give too large a value of $\sigma^{3\text{-body}}$. Inclusion of the S-wave final-state interaction may produce a better value for $\sigma^{3\text{-body}}$.

The σ_{int} for H^2 and He^4 are experimentally 30% and 58% greater than 60 (NZ/A) MeV mb. Assuming an average value of 44% for He^3, one gets

$$\sigma_{\text{int}}^{\text{total}}=40(1+0.44)=57.6\text{ MeV mb}.$$

Since this experiment has found $\sigma_{\text{int}}^{2\text{-body}}=16.5$ MeV mb (up to 40 MeV) (assuming the Gorbunov angular

[34] L. N. Hand, D. G. Miller, and R. Wilson, Rev. Mod. Phys. **35**, 335 (1963).
[35] H. Collard, R. Hofstadter, A. Johansson, R. Parks, M. Ryneveld, A. Walker, M. R. Yearian, R. B. Day, and R. T. Wagner, Phys. Rev. Letters **11**, 132 (1963).
[36] L. I. Schiff, H. Collard, R. Hofstadter, A. Johansson, and M. R. Yearian, Phys. Rev. Letters **11**, 387 (1963).
[37] B. K. Srivastava, Phys. Rev. **133**, B545 (1964).
[38] P. O. Davey and H. S. Valk, Phys. Letters **7**, 335 (1963).
[39] T. K. Radha and N. T. Meister, Phys. Rev. **136**, B388 (1964).

TABLE II. Values of the sum rules from integrating photodisintegration theories.

Ground-state wave function	Radius parameters He^3	Radius parameters H^2	Limit (MeV)	Sum rules σ_{int}^2	Sum rules σ_{int}^3 (MeV mb)	Sum rules σ_{int}^{total}	Sum rules σ_b^2	Sum rules σ_b^3 (mb)	Sum rules σ_b^{total}
Gaussian[a]	$\mu=0.2716$ F^{-1}	$\mu=0.3042$ F^{-1}	∞	26	143	169			
			40	17			0.75		
Irving $(n=0)$[b]	$\beta=0.898$ F^{-1}	$\alpha=0.2317$ F^{-1}	40	54			2.9		
Irving $(n=\frac{1}{2})$[c]	$\mu=0.357$ F^{-1}		40	14	74	88	1.0	3.8	4.8
Delves[d]	$R=2.5$ F		40		100			6.3	
Eichmann[e]	$C_1=0.3$ F^{-2}		40	16			0.96		
	$C_2=0.07$ F^{-2}								

[a] See Refs. 18 and 23.
[b] See Refs. 19 and 23.
[c] See Ref. 18.
[d] See Ref. 21.
[e] See Ref. 20.

distribution), one might expect $\sigma_{int}^{3\text{-body}}$ to be $\sim$40 MeV mb.

D. Experimental Values of σ_{int} and σ_b

Of all the experiments on the photodisintegration of He^3 in the giant resonance region, only the experiment of Gorbunov and Varfolomeev[13] has enough information to compare directly with the sum rules. These authors obtained experimentally,

$$\sigma_{int}=\int_0^{170}(\sigma_2+\sigma_3)dE_\gamma,$$

$$=(26.5\pm1.3)+(43.6\pm2.7)=70\pm3 \text{ MeV mb},$$

$$\sigma_b=\int_0^{170}\left(\frac{\sigma_2}{E_\gamma}+\frac{\sigma_3}{E_\gamma}\right)dE_\gamma,$$

$$=(1.34\pm0.05)+(1.42\pm0.07),$$

$$=2.76\pm0.08 \text{ mb}.$$

Since the angular distribution of the two-body breakup indicates appreciable electric quadrupole ($E2$) contribution to the absorption cross section, this quantity should be removed before comparing the experimental results with the calculations summarized in Tables II and III. Using the coefficient of the pure quadrupole terms in the $d\sigma_2$ angular distribution, Gorbunov and Varfolomeev calculate a $11\pm4\%$ $E2$ contribution to $d\sigma_2$. However, the coefficient of the $E1$-$E2$ interference term indicates an $E2$ contribution of only 2.2%. These are rough estimates in any case, since one would not expect the angular distribution to be independent of excitation energy. Assuming that the $E2$ contribution to $d\sigma_3$ is the same as to $d\sigma_2$, the adjusted experimental values of the electric dipole sum rules are given in Ref. 13 as $(\sigma_{int})_{E1}=62\pm5$ MeV-mb, and $(\sigma_b)_{E1}=2.53\pm0.12$ mb.

The present experiment yields the following partial sum-rule values (assuming Gorbunov's angular distribution):

$$\int\sigma^{2\text{-body}}dE_\gamma=16.5\pm10\% \text{ MeV mb},$$

$$\int\frac{\sigma^{2\text{-body}}}{E_\gamma}dE_\gamma=1.07\pm10\% \text{ mb}.$$

A reliable value of $\sigma^{3\text{-body}}$ cannot be found from this experiment. However, the results indicate that the Gunn and Irving $\sigma^{3\text{-body}}$ does not fit the three-body proton-spectrum data, whereas the $\sigma^{3\text{-body}}$ found by Gorbunov does fit fairly well.

TABLE III. Evaluations of electric dipole sum rules for He^3 and H^3.

Limit	Reference	Type	$\int\sigma dE_\gamma$ (MeV mb)	$\int\frac{\sigma}{E_\gamma}dE_\gamma$ (mb)
∞		Classical TKR	40	
∞	R[a]	Central forces	58	1.32
∞	MMR[b]	Hard core	63	2.85
∞	DV[c]	Repulsive core and/or tensor forces	65	2.36
150 MeV	GGT[d]	Dispersion relation	58	
∞	DV[e]	Analysis of electron scattering data		1.99
∞	S[f]	Analysis of electron scattering data		3.00

[a] Reference 26.
[b] Reference 27.
[c] Reference 29.
[d] Reference 30.
[e] Reference 38.
[f] Reference 37.

ACKNOWLEDGMENTS

The authors wish to thank the entire staff of the Electron Accelerator Laboratory for their assistance in the successful completion of this experiment. Particular thanks should be given to Philip Jewett and the accelerator crew for many weeks of satisfactory operation. Grateful appreciation is expressed to Barry Liles for construction of the thick Li-drifted detector used.